



Article

Study of the Decomposition of N-Nitrosornicotine (NNN) under Inert and Oxidative Atmospheres: Effect of the Addition of SBA-15 and MCM-41

Javier Asensio ¹, María Isabel Beltrán ^{1,2}, Nerea Juárez-Serrano ¹ , Deseada Berenguer ¹
and Antonio Marcilla ^{1,2,*} 

¹ Institute of Chemical Process Engineering, University of Alicante, San Vicente del Raspeig, 03690 Alicante, Spain

² Department of Chemical Engineering, University of Alicante, San Vicente del Raspeig, 03690 Alicante, Spain

* Correspondence: antonio.marcilla@ua.es

Abstract: Nowadays, the use of tobacco biomass as an energy source is being valued. Therefore, it is important to know the processes that take place during combustion and pyrolysis, as well as the substances that are formed. In this work, we study the compounds obtained during the decomposition of NNN as a function of temperature under inert and oxidant atmospheres. Moreover, the effect of the addition of SBA-15 and MCM-41 is analyzed. Two different techniques, i.e., TG/FTIR (low heating rates) and EGA Py/GC/MS (high heating rates), are used. At low temperatures NNN is almost unaltered, but it is volatilized and dragged by the carrier gas. When increasing the temperature, decomposition takes place, with pyridines being one of the most abundant compounds observed. The main compound obtained during the pyrolysis are 3- pyridinecarbonitrile, myosmine and nornicotine, which are precursors of NNN. When NNN is mixed with SBA-15, the decomposition of the NNN nitrosamine is favored at low temperatures where the yield in pyridine compounds increases. The catalysts modify the temperature and intensity of the processes, especially under an oxidative atmosphere where the residue is oxidized, showing a third loss of weight. These materials modify the compositions of gases, mainly under an O₂ atmosphere (3-pyridinecarbonitrile and myosmine showed the major effect). SBA-15 with fibrous morphology obtains the best reductions at pyrolysis conditions.

Keywords: NNN; nitrosamine; pyridines; SBA-15; MCM-41; pyrolysis; mesoporous catalysts; EGA/Py/GC/MS



Citation: Asensio, J.; Beltrán, M.I.; Juárez-Serrano, N.; Berenguer, D.; Marcilla, A. Study of the Decomposition of N-Nitrosornicotine (NNN) under Inert and Oxidative Atmospheres: Effect of the Addition of SBA-15 and MCM-41. *Appl. Sci.* **2022**, *12*, 9426. <https://doi.org/10.3390/app12199426>

Academic Editor: Leonarda Francesca Liotta

Received: 31 August 2022

Accepted: 15 September 2022

Published: 20 September 2022

Publisher's Note: MDPI stays neutral with regard to jurisdictional claims in published maps and institutional affiliations.



Copyright: © 2022 by the authors. Licensee MDPI, Basel, Switzerland. This article is an open access article distributed under the terms and conditions of the Creative Commons Attribution (CC BY) license (<https://creativecommons.org/licenses/by/4.0/>).

1. Introduction

Currently, the fact that smoking is strongly related to lung cancer and other deceases is known everywhere. However, many people are not aware of the amount of substances present in tobacco (or generated in the smoking process) that have cancerogenic effects [1–3]. Cigarette smoke presents more than 8000 different compounds [4], and it is likely that this number could still increase. At least 250 are known to be highly toxic and harmful, including hydrogen cyanide, carbon monoxide or ammonia, and 69 compounds have confirmed carcinogenic activity in humans [5,6].

Due to this, with the aim of reducing tobacco consumption and, at the same time, trying to maintain the economic value of the companies that produce tobacco, work is being performed on the possibility of promoting the role of tobacco as a source of biomass in the production of medicine [7], cosmetics [8] or energy [9]. The studies carried out to date and the new studies focused on the characterization and behavior of tobacco components can help to achieve a better guide in this new application.

Nitrosamines are organic molecules including the N-nitroso functional group. Different nitrosamines can be found in tobacco smoke, both in the gas phase and in the particulate phase. TSNAs in tobacco smoke are frequently classified into three groups regarding their chemical nature: volatile nitrosamines (VNAs), nonvolatile nitrosamines (NVSAs) and tobacco-specific nitrosamines (TSNAs).

Tobacco-specific nitrosamines (TSNAs) are one of the most important groups of carcinogens in tobacco products (Hoffmann and Hecht include them in their list of tumoral agents in tobacco smoke several VNAs [10]). They are principally formed by the nitrosation of the alkaloids present in the tobacco plant [11].

Most of the nitrosamines cause mutations in DNA and are carcinogenic to humans, with the nitrosamines NNK (nitrosamine ketone derived from nicotine) and NNN (nitrosonornicotine) being the ones with the highest risk [12,13].

Normally, only a little portion of TSNAs is generated during the smoking process. The major portion of the TSNA is generated during the curing process, and it is transferred into tobacco smoke as preformed TSNA [14]. They can be formed by a pyrosynthesis process from the tobacco alkaloids acting as precursors. Nornicotine, anabasine and anabutine are precursors of NNN, NAB, NAT and NNK, and nicotine is also a precursor of NNK and NNN [15]. It is generally accepted that NNN is formed via the nitrosation of nornicotine, a secondary alkaloid generated directly from nicotine through activity of the enzyme nicotine demethylase. NNK is formed from the nitrosation of nicotine or its oxidized products [16].

In the formation process of nornicotine, anabasine and anabutine, these molecules suffer an oxidative N-nitrosation of the secondary amines. According to Hecht et al. [17], NNK is formed through the oxidative N-nitrosation of the tertiary amine of the nicotine followed by the opening of C2' ring and the pyrrolidine ring.

Adams et al. [18] concluded that around 6.9–11% of the NNK formed as a consequence of the curing process passes to the smoke during smoking, representing 26–37% of the total NNK detected. Brunnemann and Hoffmann [19] have analyzed the amounts of four TSNAs in the smoke of different tobaccos. They found amounts ranging from 113 to 788 ng/cigarette total TSNAs.

The use of zeolites and other mesoporous and microporous aluminosilicates as zeolite NaA, NaY, ZSM-5, SBA-15 and MCM-48 has been studied for removing nitrosamines from the air [20–22] and water [23,24]. Factors such pore size, surface area, morphology and interaction among the functional groups of the nitrosamines and the adsorbents have significant influences on the process.

Removing nitrosamines from the tobacco smoke is a more complicated process, since TSNAs are heavier and are part of the particulate matter, whose particle size is larger than the materials pore diameter [24]. However, Gao et al. [25] found that the CAS-1 calcsilicate removes among 30–60% of TSNAs from the smoke, whereas materials such as NaA zeolite being very effective in removing nitrosamines from air streams, hardly reduced 11% of TSNAs from tobacco smoke. They explained such results being because the fiber morphology of the calcsilicate favors the collision of the particulate matter.

Lin et al. [26] highlighted the ability of SBA-15 and NaY zeolite for removing the particulate matter and TSNAs, observing a certain selectivity of the SBA-15 due, again, to its fiber-like morphology. These authors also used other zeolitic catalysts in their acid and sodic forms, as well as MCM-41, for reducing TSNAs in Burley tobaccos. They also studied the decomposition of the TSNAs adsorbed on the catalysts. This study observed that the aluminosilicates were more uniformly distributed on tobacco strands due to their low apparent density. They found a 19% and 30% reduction of TPM and 22% and 35% TSNAs when using MCM-41 and SBA-15, respectively. However, they developed their study by adding 10 μ L of a solution with 5 mg of nitrosamine in 5 mL of methanol to 5 mg of catalyst, previously activated. Once the methanol is evaporated, the resulting concentration of nitrosamine is around 0.33 wt%. This seems a very high catalyst concentration, very far from a possible real application. Moreover, the product may result in a heterogeneous mixture, since not all the catalyst may be wet by the solution. The products were analyzed

only by GC/MS at an inert atmosphere. The experiments reported by these authors, on the decomposition of the NNN adsorbed on these catalysts, are very interesting and constitute a valuable reference for our work.

According to [27–29], the NNN pyrolysis starts by the breaking of N-NO bond, and the intermediate formed reacts through two pathways. The first is the dehydrogenation to give 3-(4,5-dihydro-3H-pyrrole-2-yl) pyridine, and the second is the methylation of the nitrogen atom of the pyridine ring to give 3-(N-methylpyrrolidine-2-yl) pyridine, that can be aromatized to produce 3-(N-methylpyrrol-2-yl) pyridine. The main product is 3-(4,5-dihydro-3H-pyrrole-2-yl) pyridine, that further decomposes to 3-vinylpyridine and 3-pyridinecarbonitrile through the breaking of the C-N and C-C bonds of the five atoms ring. In the presence of zeolites and aluminosilicates of the SBA-15 and MCM-41 type, cyanopyridine was not obtained, but quinoline and isoquinoline were observed. This indicates that the pyrrole ring has not been cracked, but has been rearranged to a more stable structure involving a benzene ring on the quinoline. According to these authors, the decomposition products are not as carcinogenic as the NNN. On another hand, they observed that the catalysts were strongly adhered to the tobacco leaf and did not pass to the smoke.

In our group, we have studied the use of aluminosilicates to reduce the toxicity of tobacco. We have also studied the effect of these catalysts on the products derived from the pyrolysis and combustion of the highly toxic compounds present in tobacco smoke. These analyses have been carried out as a function of temperature. Recently, we have studied the effect of such catalysts on different tobacco additives and nicotine [30–34].

Thus, the objective of the present work, is to study the decomposition of N-nitrosornicotine (NNN) in TG/FTIR at a slow heating rate, as well as the fast pyrolysis at different temperatures in an EGA pyrolysis equipment connected in line with a GC/MS. In this way, it is intend to evaluate the nature of the compounds generated when this nitrosamine is heated under inert and oxidizing atmospheres (He and air), emulating the processes of combustion and pyrolysis present in smoking. In addition, the effect of three mesoporous materials, SBA-15f (fiber like morphology), SBA-15p (platelet like morphology) and MCM-41, in direct contact with the NNN and under the same conditions, is studied to evaluate the modification in the compound generated during the decomposition of this nitrosamine. These catalysts have been studied in the decomposition of nicotine in a previous paper [35] (under review), and will be studied in the decomposition of NNK in a complementary work.

2. Experimental

Nitrosamine N-nitrosornicotine (NNN) with purity higher than 98% was supplied from Alfa Aesar. Then, a solution of NNN 0.5% *w/w* in methanol was prepared. A SBA-15 with a fiber-like morphology (SBA-15f) was synthesized according to the procedure described by Zhao et al. [36]. BASF P123, Tetraethyl orthosilicate (Wacker, >99% purity) and HCl (Merck 37%) were used as reactants. The SBA-15 with platelet-like morphology (SBA-15p) was synthesized according to the procedure described by Yeh et al. [37] using Cetil trimethyl ammonium bromide and sodium dodecyl sulphate (Acros Organics, >99% purity), sulphuric acid (Merck, >99% purity), sodium silicate (Schalau, neutral solution pure) and sodium hydroxide (Sigma Aldrich, >98% purity). MCM-41 was prepared as described Gaydhankar et al. [38], employing Cetil trimethyl ammonium bromide (Acros Organics, >99% purity), ammonia (merck, 25% solution) and tetraethyl orthosilicate (Wacker, >99% purity).

The catalysts obtained were characterized by N₂ adsorption isotherms (using a Quantachrome AUTOSORB-6), DRX (using a Bruker CCD-Apex, diffractometer) and electron microscopy (using a JEOL JSM-840 apparatus). The temperature-programmed desorption (TPD) of ammonia allows for the acidity of the materials to be obtained. The analysis was developed in a Netzsch TG 209 thermobalance. Maintaining a N₂ flow of 45 mL/min, the samples were heated at 500 °C with a rate of 10 °C/min. Then, the materials were cooled

to 100 °C, and a flow of ammonia of 35 mL/min was applied during 30 min. Next, in order to remove the physisorbed ammonia, a flow of 45 mL/min of N₂ was applied for 1 h, maintaining the temperature. Finally, the samples were heated to 900 °C with a rate of 10 °C/min. The acidity was quantified according to the weight loss observed in the TPD experiment. The Si/Al ratio was determined by X-ray fluorescence (XRF) in a Philips Magix PRO, model PW2400.

The characteristics of the SBA-15f, SBA-15p and MCM-41 materials are shown in Table 1 and Figures 1 and 2.

Table 1. Characteristics of catalysts obtained.

Catalyst	Pore Size (nm)	Pore Volume (cm ³ /g)	BET Area (m ² /g)	External Surface Area (m ² /g)	Acidity (mmol/g)	Si/Al Ratio (%)
SBA-15f	6.091	0.954	728.1	552.1	0	100
SBA-15p	7.244	1.281	1009	591.8	0	100
MCM-41	2.182	0.905	1154	199.3	0.42	47

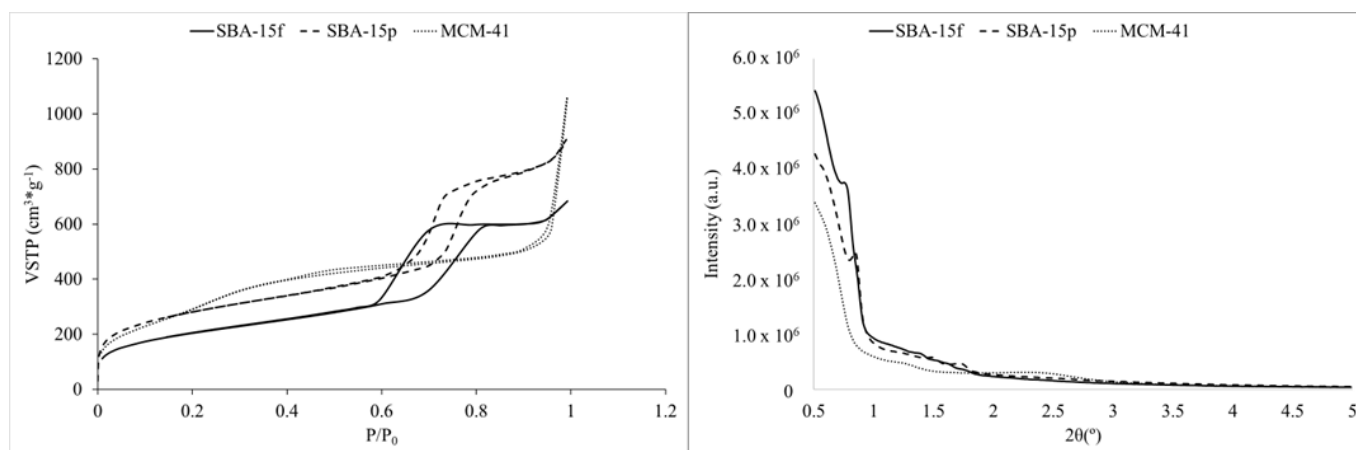


Figure 1. 77 K N₂ adsorption isotherms (left) and diffractograms (right) of the three catalysts obtained.

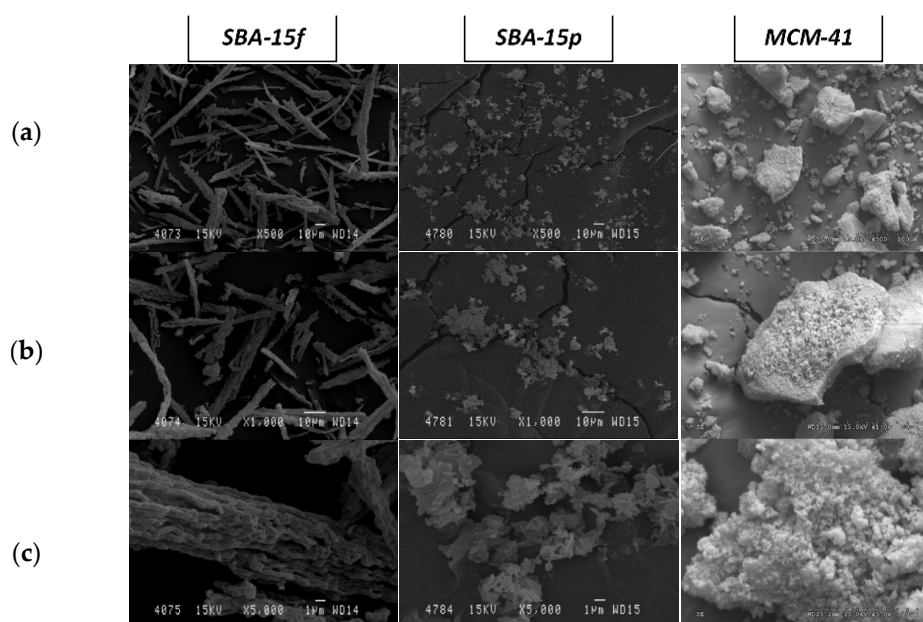


Figure 2. Electron micrographs of the SBA-15f, SBA-15p and MCM-41 at 500 (a), 1000 (b) y 5000 (c) magnifications.

The DRX diffractograms showed the typical behavior of these materials. The two SBA-15s show the diffractogram peaks (100), (110) and (200) characteristic of the P6mm symmetry [36]. The diffraction pattern of the MCM-41 obtained is also characteristic of this aluminosilicate. The morphology of these materials was observed in the SEM micrographs (Figure 2). The SBA-15 presented a fiber-like (SBA-15f) and platelet-like (SBA-15p) morphology, and MCM-41 showed the particulate aspect of this material.

TG/FTIR were run in a Mettler Toledo TGA/DSC 1 STArE coupled to a FTIR Bruker Tensor 27. The transfer line was maintained at 200 °C. The temperature program was 20 min at 40 °C, heating at 35 °C/min up to 800 °C and holding temperature during 5 min. 80 mL/min of N₂ (99.9992%) or air synthetic (21% O₂ and 79% N₂) were used as the entrained gas in the corresponding experiments. FTIR spectra were obtained at four scans per second between 600 and 4000 cm⁻¹.

The other series of experiments were carried out under flash conditions in a multi-shot pyrolyzer model EGA/PY-3030D, supplied by Frontier Laboratories, and directly coupled on a GC/MS (gas chromatograph Agilent 6890N with electron-impact mass selective detector Agilent 5973). To separate the compounds, an UA5-30M-0.25F column was used with 2 mL/min flow. The experimental conditions used were: an isothermal ramp at 45 °C during 5 min, a dynamic ramp until 285 °C at 12 °C/min and a final isothermal of 5 min, with a 50:1 split ratio. The decomposition of NNN nitrosamine was studied under two atmospheres at different temperatures. Flash pyrolysis experiments were performed in He (99.9992% purity) at 300, 400 and 500 °C, and flash oxidative experiments were performed in synthetic air (21% O₂ and 79% N₂) at 300, 325, 350, 375, 400 and 425 °C.

Afterwards, when running TG experiments, approximately 30–40 mg of this solution was placed in the sample holder and heated at 80 °C to eliminate the methanol. Operating in this way, the amount of NNN in the sample holder was around 1.5 to 2 mg. When using a catalyst, around 2 mg of catalyst was placed in the sample holder and 30–40 mg of the NNN methanol solution was added. In this way, the ration NNN/catalyst was around 1:1. In the case of EGA experiments, around 3.7 mg of the NNN/methanol solution was added. When running catalytic experiments, around 0.2 mg of catalyst was first placed in the sample holder and then the solution was added. In this case, the NNN/catalyst ratio was around 1/11. The sample holder was heated to 80 °C to remove the methanol and then kept in a cold area. The equipment was heated at the selected temperature, and the sample was introduced into the oven and maintained at this temperature during 0.2 min. Finally, the compounds generated were separated by GC and detected by MS. This procedure was used in the presence and absence of catalysts, so that the results were not affected by the sample preparation method.

3. Results and Discussion

3.1. TG/FTIR Experiments

Figure 3 shows the TG and DTG traces of the NNN and the NNN with the three catalysts, performed under inert atmosphere.

Data below 100 °C are not shown because they correspond to the loss of water in the samples with the catalyst. Data under an inert atmosphere corresponding to sole NNN present a wide process with a peak at 190 °C and a shoulder at around 183 °C. Another shoulder, more marked, can be observed at 218 °C, as a result of NNN volatilization and decomposition. When using the two SBA-15 catalysts, the main peak is shifted to higher temperatures (267 °C), and another minor peak at 155 °C and a marked shoulder at 197 °C are observed. The first processes observed may correspond to the volatilization and decomposition of NNN that does not interact or interacts weakly with the catalyst (this peak is slightly more marked for the SBA-15f), whereas the main peak must be the result of the NNN adsorption in the catalyst pores and the further decomposition of the catalyst's pore structure. MCM-41 produces more marked changes, and up to four processes can be observed. At low temperatures, a shoulder at 155 °C and a peak at 176 °C, followed by other at 197 °C, can be observed. These two peaks are much more intense than those

observed with the SBA-15 catalysts. The main peak appears at 247 °C, being lower than in the case of the other catalysts and presenting a tail at high temperatures.

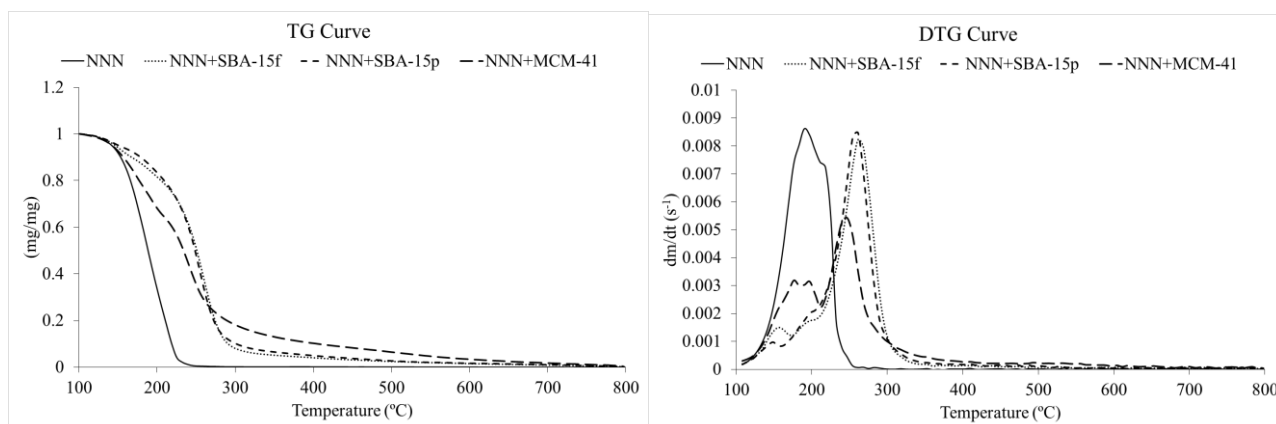


Figure 3. TG and DTG curves for experiments with NNN and NNN with three catalysts under inert atmosphere.

These changes, compared with the experiment without a catalyst, may be related to the interaction between the NNN and the different porous structures of these materials. The first peaks that appear in the presence of the catalyst below 200 °C are similar to those presented by NNN when it is alone, and could be due to the evaporation and partial decomposition of the nitrosamine that has not interacted with the catalyst. The rest of the NNN that decomposes at higher temperatures is probably retained in the pores of the catalysts or has been adsorbed on their external surface. According to the intensity of the main peaks of the DTG, the amount of NNN adsorbed would be higher for the SBA-15, which is consistent with its larger pore volume and external surface area.

These peaks at a low temperature will be in good agreement with the results of the pyrolysis in the EGA equipment, where the decomposition of the NNN in the presence of catalysts is observed at lower temperatures, especially in the case of MCM-41.

Under the air atmosphere (Figure 4), the results of sole-NNN are very similar to those under inert conditions, showing very little influence of the atmosphere on the thermal behavior of NNN. When using the catalyst, the first part of the thermogram is also very similar to that in N_2 , but from temperatures around 290 °C a significant residue is obtained (i.e., around 15%) that decomposes at an almost constant rate up to 700 °C. Again, the traces corresponding to the two SBA-15s are very similar, and the greatest differences are produced by the MCM-41. In this case, a much more pronounced residue is obtained that oxidizes at temperatures between 500–700 °C.

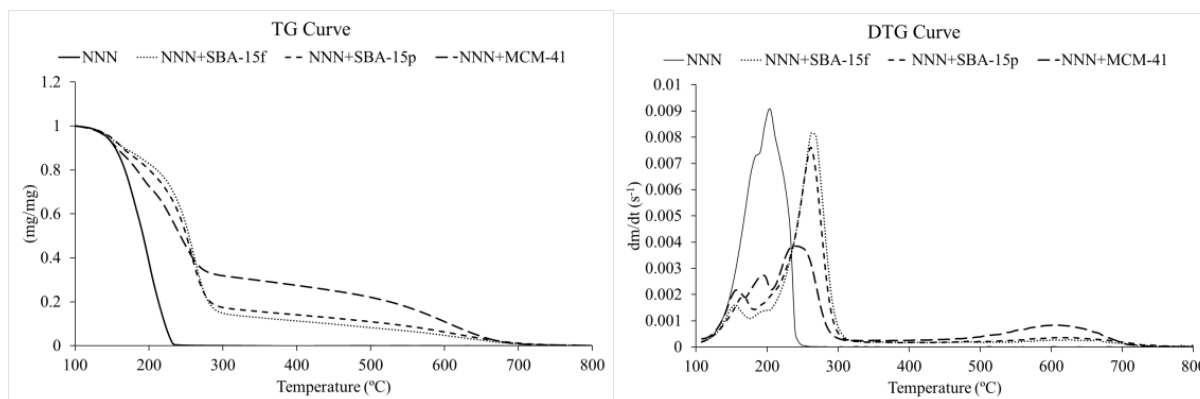


Figure 4. TG and DTG curves for experiments with NNN and NNN with three catalysts under oxidizing atmosphere.

The IR data under the inert atmosphere show a very poor resolution, and only the bands corresponding to NO at 1906 and 1842 cm^{-1} and those corresponding to CN (triple bond) at 2229 cm^{-1} can be hardly observed, being slightly more intense when using the catalyst. Nevertheless, the data show no conclusive differences.

Under the air atmosphere, the IR spectra show higher differences (Figure 5), mainly with respect to the bands corresponding to CO at 2193 cm^{-1} and CO₂ at 2351 cm^{-1} . The peaks around 250 °C are of similar intensity for the 2351 cm^{-1} band, and the presence of catalysts provoke their appearance at lower temperatures in both bands. During the second interval, at temperatures around 570 °C, a very intense signal is observed in the 2351 cm^{-1} (CO₂) band. This signal is enhanced mainly by the presence of MCM-41 and followed by the two SBA-15s, presenting less (or negligible) intensity in the experiment without a catalyst. A similar behavior is observed for 2193 cm^{-1} band. This fact could confirm the higher generation of carbonaceous residue in the presence of MCM-41, which is oxidized at high temperatures in an oxidizing atmosphere. MCM-41 also produces a large peak of aromatic C-H band (700 cm^{-1}) at high temperatures and presents a lower intensity of the peaks of the R-O bands at 1238 cm^{-1} , C=C at 1468 cm^{-1} and NO at 1913 cm^{-1} . Nevertheless, the information provided by this technique is very limited and much more interesting results are obtained by EGA, where the composition of the gases evolved can be obtained.

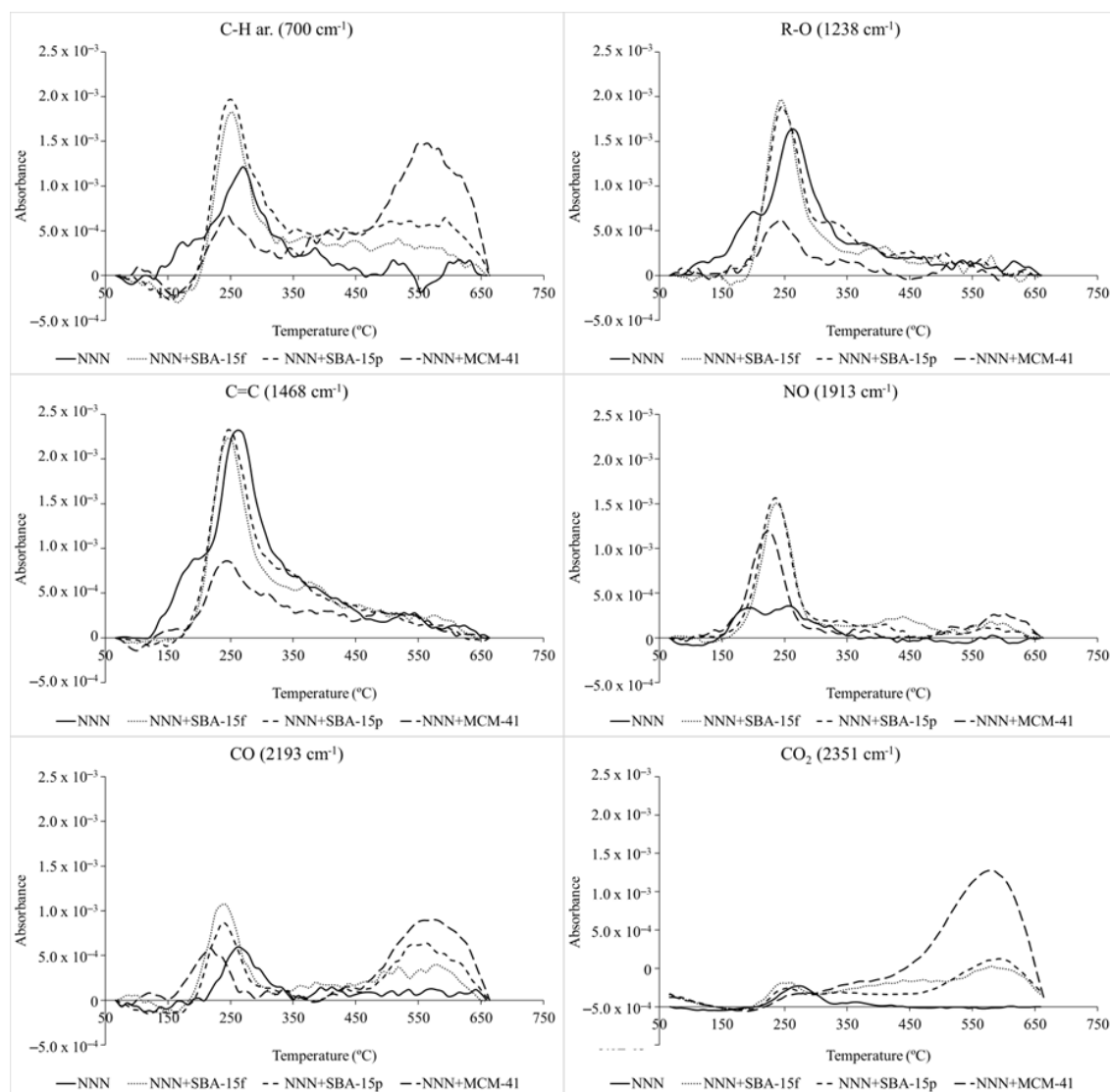


Figure 5. IR spectra of NNN and NNN with three catalysts, under oxidizing atmosphere.

3.2. EGA Fast Pyrolysis of Sole NNN

Figure 6 shows the spectra obtained at the three temperatures studied for NNN in the He atmosphere. As can be seen, at 300 °C the chromatogram presents two major peaks where the largest corresponds to NNN (at around 18 min retention time). When the temperature increases, the intensity of the NNN peak decreases, disappearing at 500 °C. The peak of myosmine (at around 15 min retention time) presents a maximum at 400 °C, whereas the other peaks observed increase their intensity with increasing temperature.

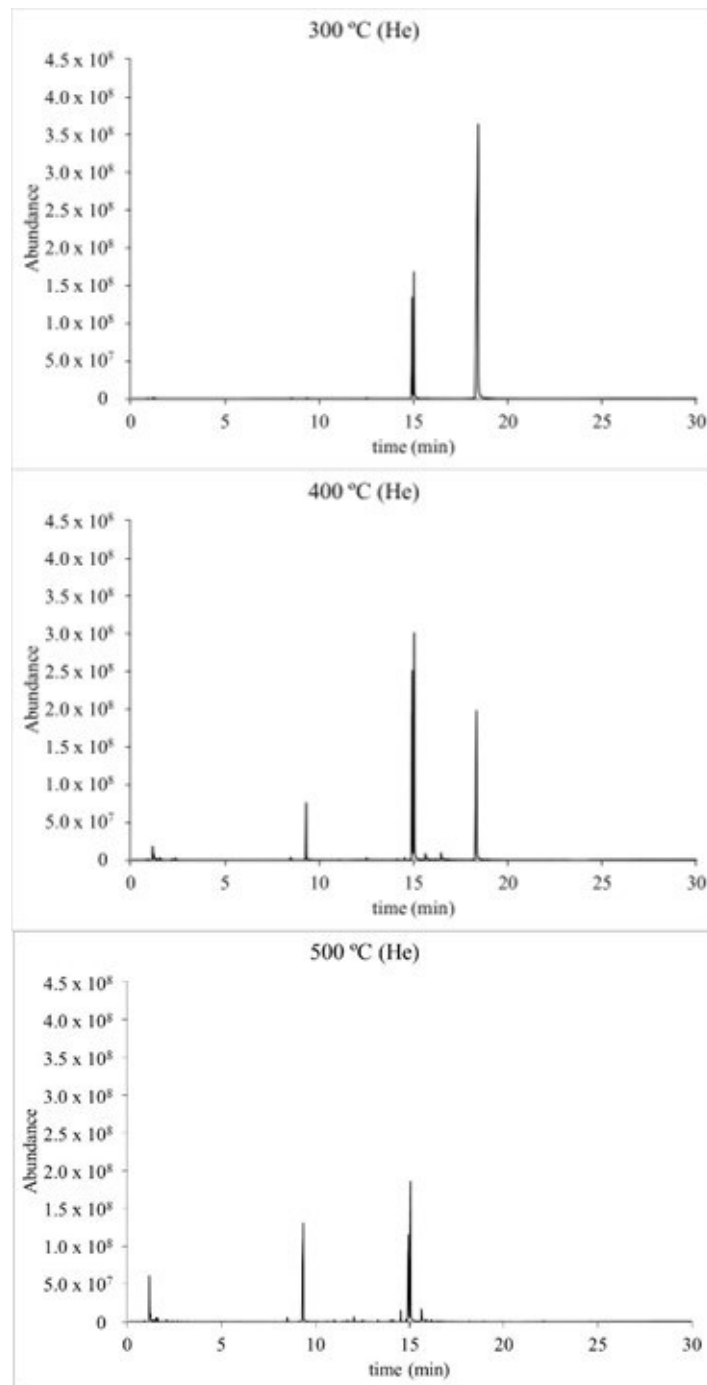


Figure 6. Chromatograms of the pyrolysis of NNN at different temperatures under the He atmosphere.

Figure 7 shows the spectra obtained for NNN in the air atmosphere at the six temperatures studied.

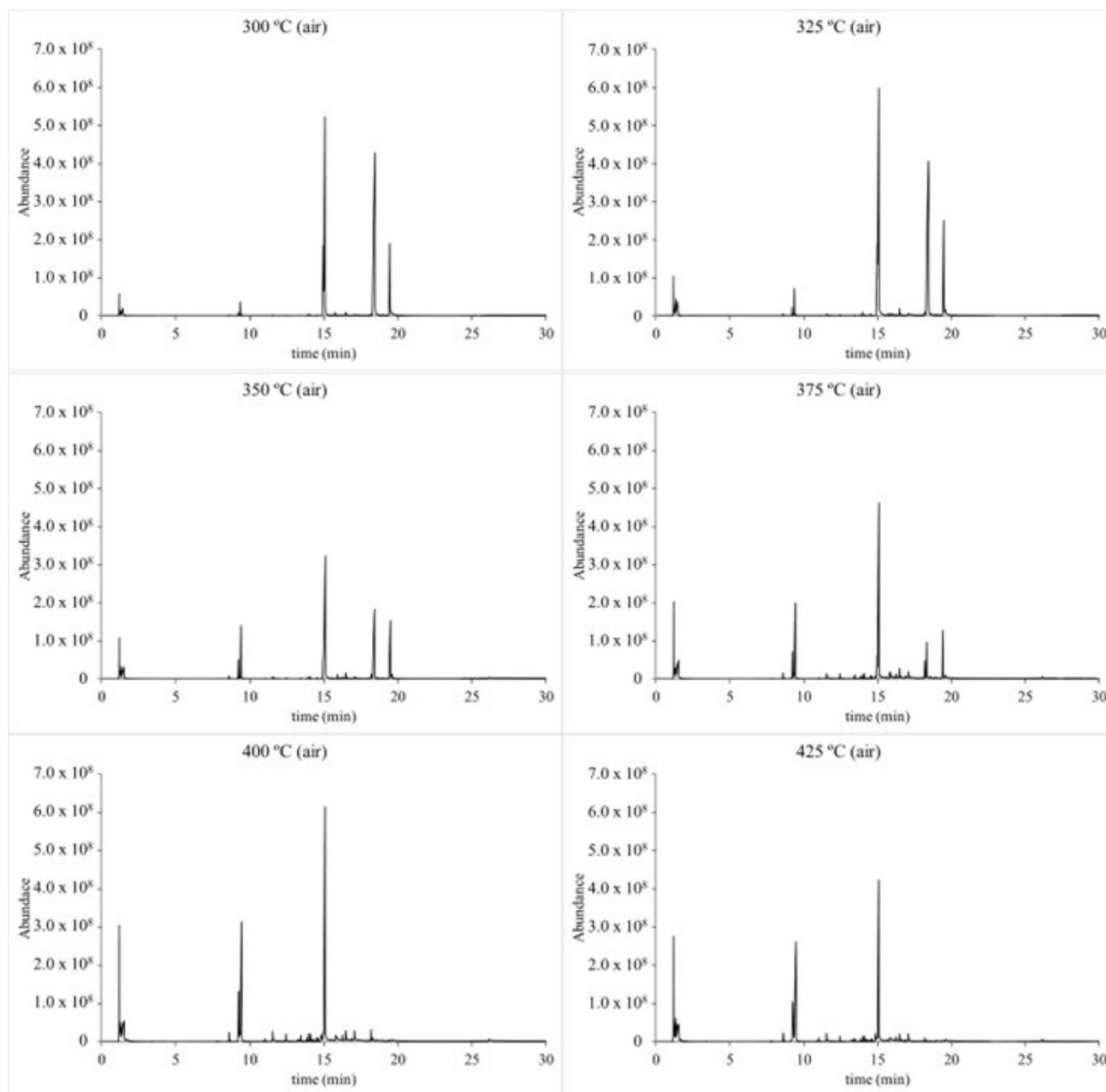


Figure 7. Chromatograms of the pyrolysis of NNN at different temperatures under the air atmosphere.

Under air atmosphere, the NNN (18 min) is less stable and the peak of myosmine (15 min) at 300 °C is already the major peak. At 400 °C the NNN has almost disappeared. Under He atmosphere, 94 peaks have been assigned, and 93 under air atmosphere. Appendix Table A1 shows the list of compounds assigned in all experiments that represent more than 0.5% area and have a match-quality factor higher than 80%. We assigned 1H-pyrrol [2,3-b] pyridine and 5,6 dimethyl-3H Pyrrol [2,3-b] pyridine by interpreting their mass spectra and considering the probability of obtaining such structures from the NNN pyrolysis.

Figure 8 shows the evolution of the % area of NNN versus temperature for the two atmospheres. It can be seen that the NNN is more stable in the He atmosphere than in air, showing a marked degradation at 300 °C under oxidizing conditions.

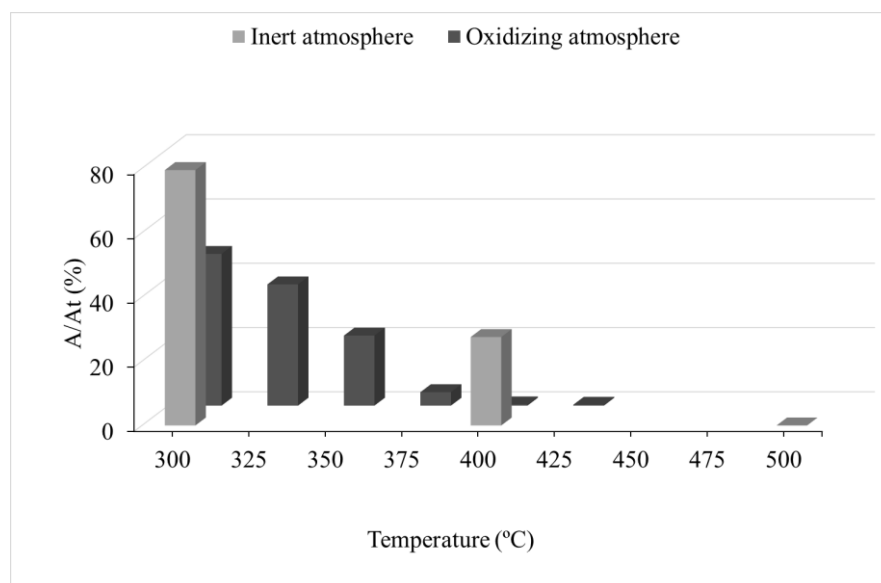


Figure 8. Evolution of NNN with temperature in the He and air atmospheres.

Figure 9 shows the evolution of the main compounds detected under inert conditions versus temperature. Myosmine (compound number 29) is the main compound at the three temperatures considered, reaching a yield of around 27% at 400 and 500 °C. 3-pyridincarbonitrile (compound 13) is the second major compound at 500 °C, and presents a marked increase with temperature reaching 23%. 1H-pyrrolo [2,3-b] pyridine (compound 27) levels its yield at 400 °C at 12.7%. Nornicotine (compound 28) and nornicotyrine (compound 34) present a maximum yield at 400 °C, as a consequence of their first formation from NNN and the subsequent pyrolysis reactions they undergo. 3-ethenylpyridine, 3-pyridinecarbonitrile, isoquinoline, nicotine, myosmine, nicotyrine and nornicotyrine were also detected by Zhu et al. [26], who also obtained myosmine and 3-pyridinecarbonitrile as the majority compounds when studying the degradation of NNN.

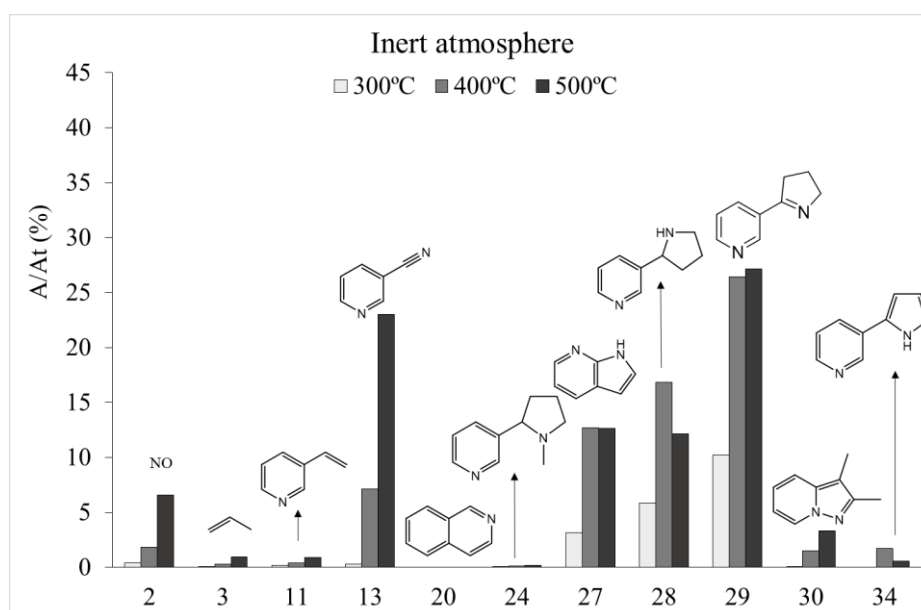


Figure 9. % area vs temperature of the majority compounds detected in the pyrolysis of NNN under inert atmosphere. Nitric oxide (2), 1-propene (3), 3-ethenyl-pyridine (11), 3-pyridinecarbonitrile (13), isoquinoline (20), nicotine (24), 1H-pyrrolo [2,3-b] pyridine (27), nornicotine (28), myosmine (29), 3,4-dimethyl-pyrrolo(1,2-a) pyrazine (30), nornicotyrine (34).

Figure 10 shows the evolution of the products obtained under the air atmosphere as a function of temperature.

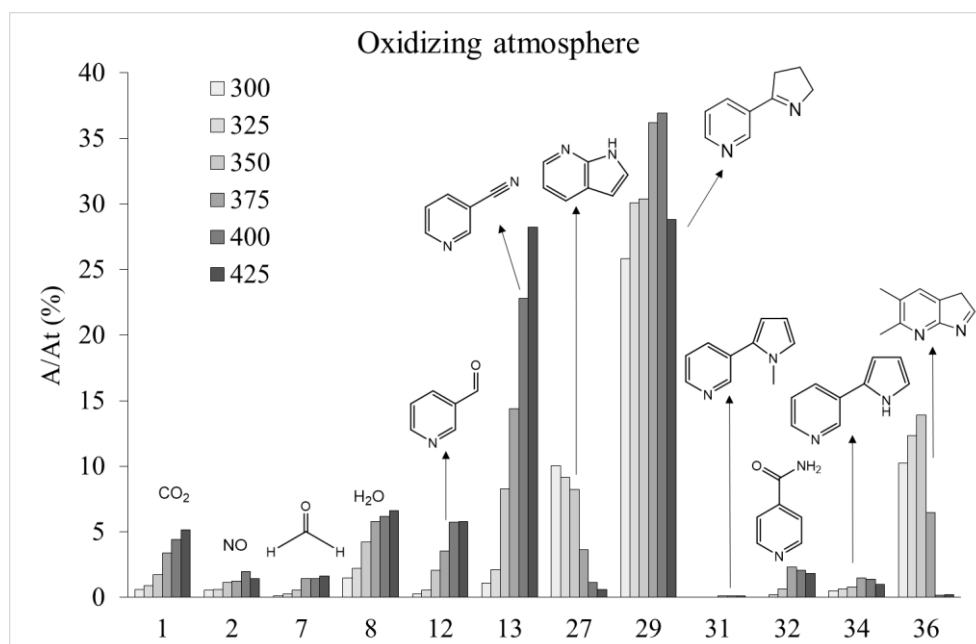
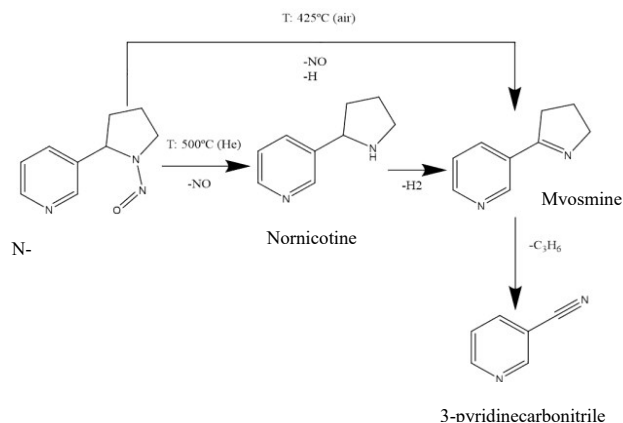


Figure 10. % area vs temperature of the majority compounds detected in the pyrolysis of NNN under air atmosphere. Carbon dioxide (1), nitric oxide (2), formaldehyde (7), water (8), 3-pyridinecarboxaldehyde (12), 3-pyridinecarbonitrile (13), 1H-pyrrolo [2,3-b] pyridine (27), myosmine (29), nicotirine (31), 4-pyridinecarboxamide (32), normicotirine (34) y 5,6-dimethyl-3H-pyrrolo [2,3-b] pyridine (36).

Myosmine (compound 29, that reached around 37% of the total area at 400 °C) and 3-pyridinecarbonitrile (compound 13, that represents 28% at 425 °C), are the main compounds, as observed under the inert atmosphere. Nevertheless, their behavior is somewhat different, since myosmine presents a maximum with temperature while 3-pyridinecarbonitrile shows an increasing trend with temperature throughout the range studied. Carbon dioxide (compound 1) and water (compound 8) also present an increasing trend with temperature reaching 5 and 6.6% respectively, at 425 °C. Nicotirine (compound 31) is practically not observed, contrarily to the case of the pyrolysis of nicotine and NNK [39]. Some of the detected compounds decrease when increasing temperature, as is the case of 1H-pyrrolo [2,3-b] pyridine (compound 27) that presents its major contribution at 300 °C.

According to Zhu et al. [26], the majority compounds detected can be formed via the Scheme 1.



Scheme 1. Possible route for the formation of the majority compounds in NNN pyrolysis.

Under oxidizing conditions, nornicotyrine is much more reactive and is hardly detected.

3.3. Catalytic Pyrolysis of NNN in the Presence of Mesoporous Silicates

3.3.1. Catalytic Pyrolysis under Inert Atmosphere

When NNN was mixed with SBA-15f, SBA-15p and MCM-41, the chromatograms showed important changes (Figure 11).

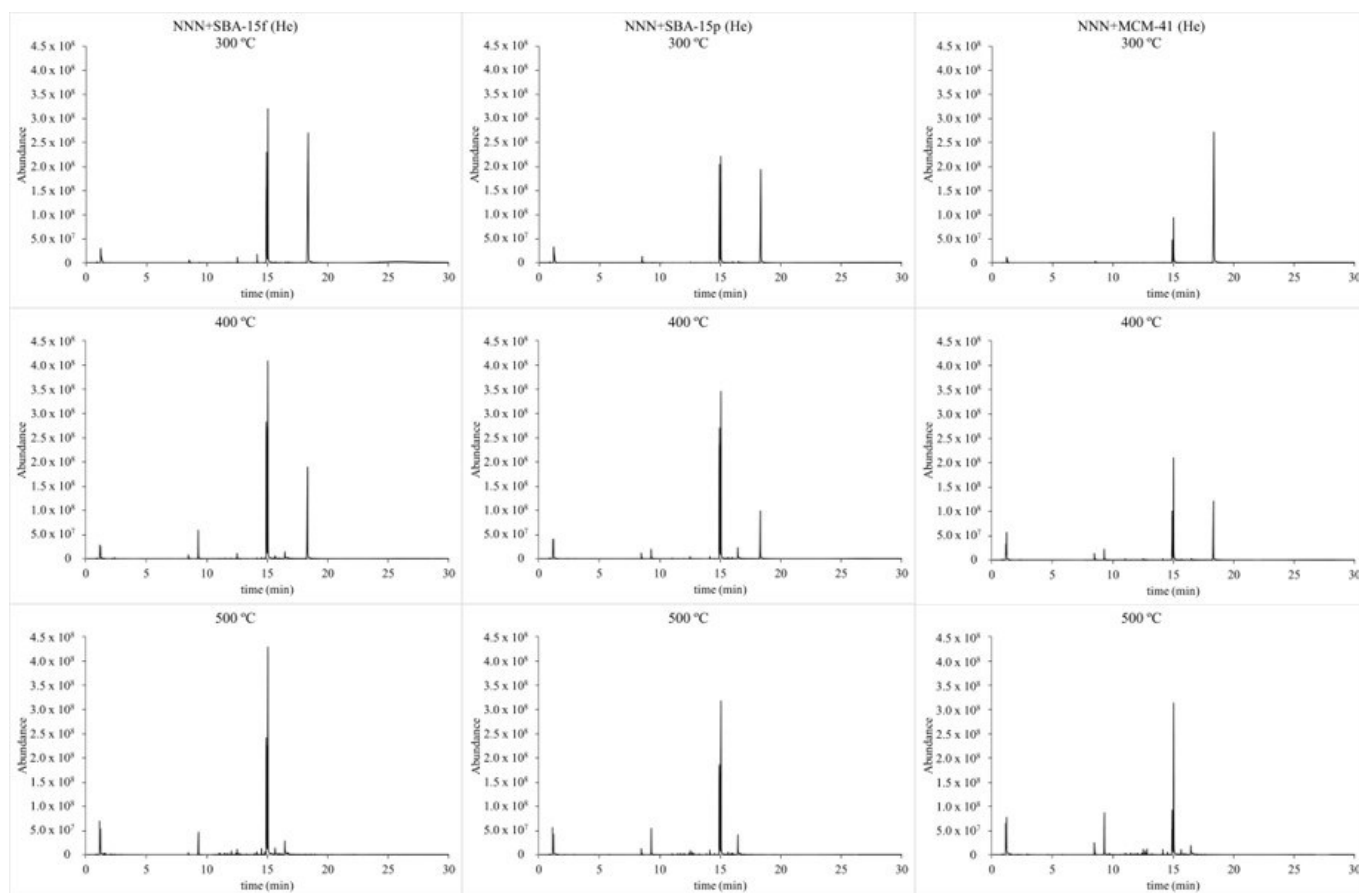


Figure 11. Chromatograms of the pyrolysis of NNN with SBA-15f (**left**), SBA-15p (**center**) and MCM-41 (**right**) at different temperatures under the He atmosphere.

In general, the same peaks observed in Figure 6 are present in these chromatograms. Nevertheless, new peaks appear.

Appendix Table A2 shows the % area of the peaks presenting a % area > 0.5 and a match quality > 80% for the three catalysts at the three temperatures studied.

Figure 12 shows the evolution of NNN with temperature. At low temperatures, a greater decomposition than in the case of sole-NNN can be observed when the catalysts were employed. In accordance with Zhu et al. [40,41], both SBA-15s have a pore size large enough to adsorb the NNN and promote its decomposition. MCM-41 produces an intermediate degradation of the NNN, generating a larger amount of residue. This is due to its lower pore size but higher surface area and its accessibility to the porous structure facilitated by its morphology.

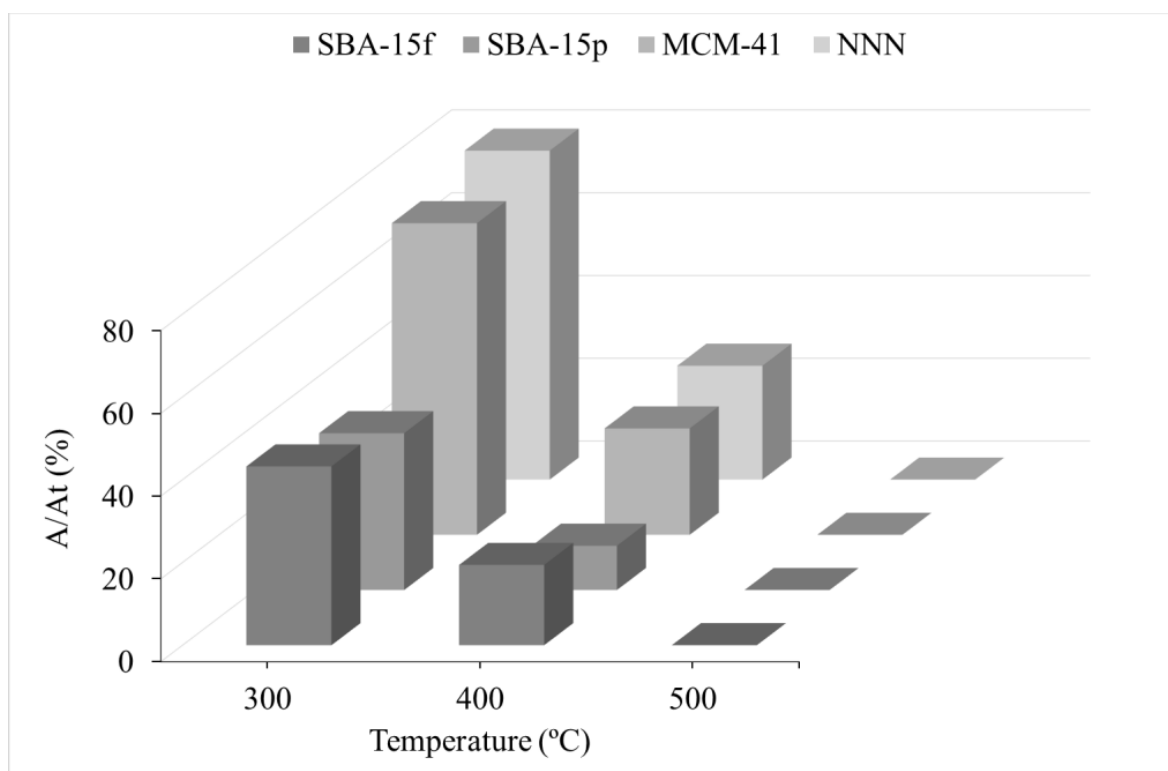


Figure 12. Evolution of NNN for sole NNN and NNN with three catalysts under the inert atmosphere.

Figure 13 shows the contribution to the total area of the products considered (i.e., those having a % area > 0.5 and a match quality > 80%).

The sum of the contributions of all considered peaks seems to follow the order SBA15f > SBA-15p > MCM-41, thus the remaining residue must follow the order inverse, in good agreement with the residues observed in TG experiments.

The three catalysts increase most of the observed products, such as normicotine (compound 28), myosmine (compound 29) and normicotirine (compound 34). Myosmine from sole NNN pyrolysis at 500 °C was 27% and reached around 43% for the two SBA-15s and 40% for MCM-41. Contrarily, the three catalysts reduced around 50% the formation of 3-pyridinecarbonitrile (compound 13) at 500 °C.

Catalysts increase nitrogen oxide (compound 2) at 300 and 400 °C and decrease its formation at 500 °C. These results are in concordance with the data obtained by Wei et al. [26] who studied the decomposition of NNN under inert conditions. They showed that the degradation of NNN begins with the breaking of the N-NO bond, leading to the formation of nitrogen oxides and normicotine that can decompose into less or non-carcinogenic compounds. In addition, the authors observed that, during the decomposition of NNN, the products nitrosamine, nicotinonitrile and 4-ethenyl-pyridine were generated, but, in the presence of SBA-15, these compounds decreased. Moreover, the presence of SBA-15 greatly increased the yield of myosmine and favored the formation of new compounds, such as nicotyrine [26,42].

3.3.2. Catalytic Pyrolysis under Oxidizing Atmosphere

Figure 14 shows the results obtained for the analysis under the air atmosphere.

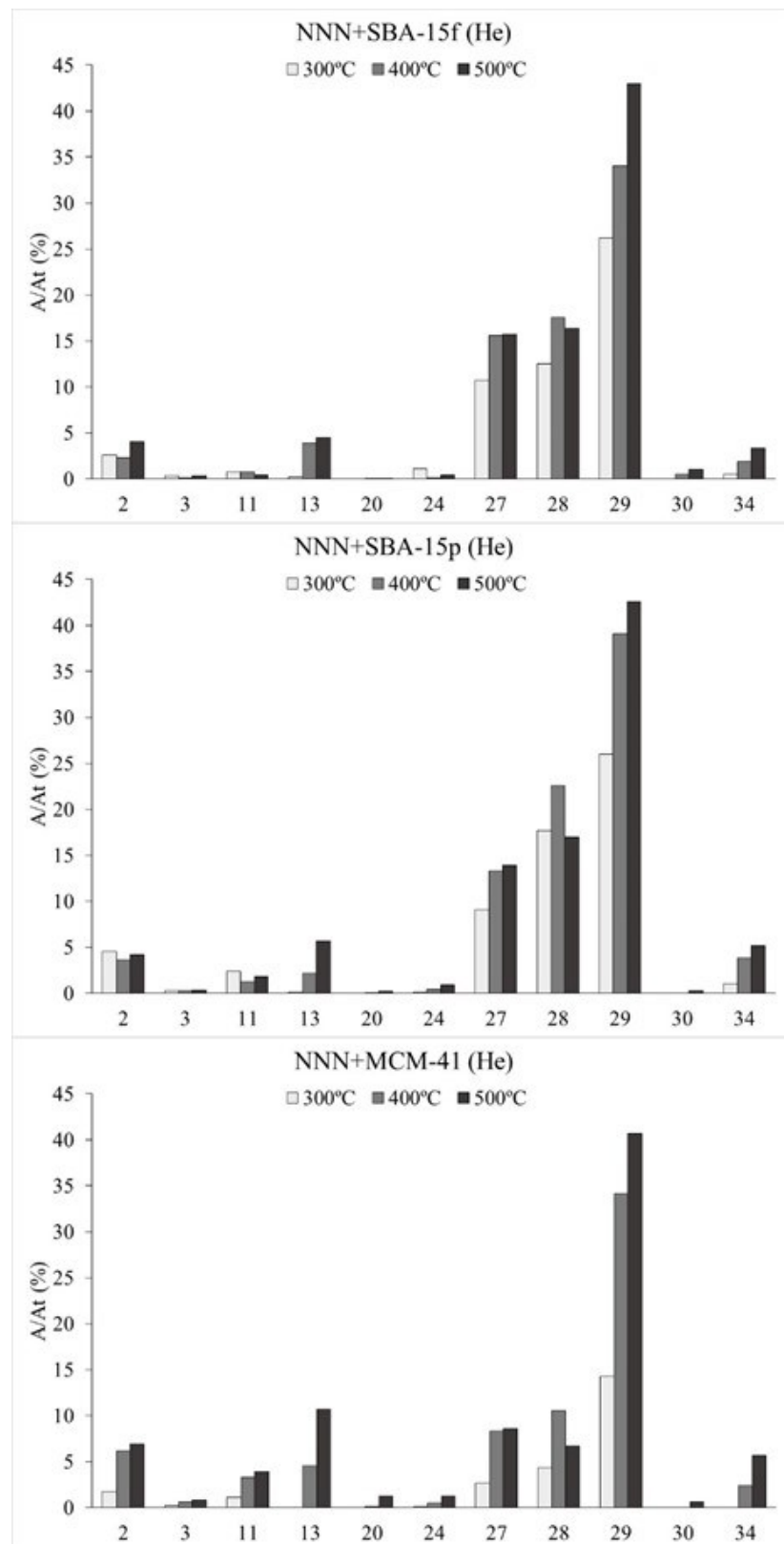


Figure 13. % area vs temperature of the majority compounds detected in the pyrolysis of NNN with three catalysts, under the inert atmosphere. Nitric oxide (2), 1-propene (3), 3-ethenyl-pyridine (11), 3-pyridinecarbonitrile (13), isoquinoline (20), nicotine (24), 1H-pyrrolo [2,3-b] pyridine (27), nornicotine (28), myosmine (29), 3,4-dimethyl-pyrrolo(1,2-a) pyrazine (30), nornicotirryne (34).

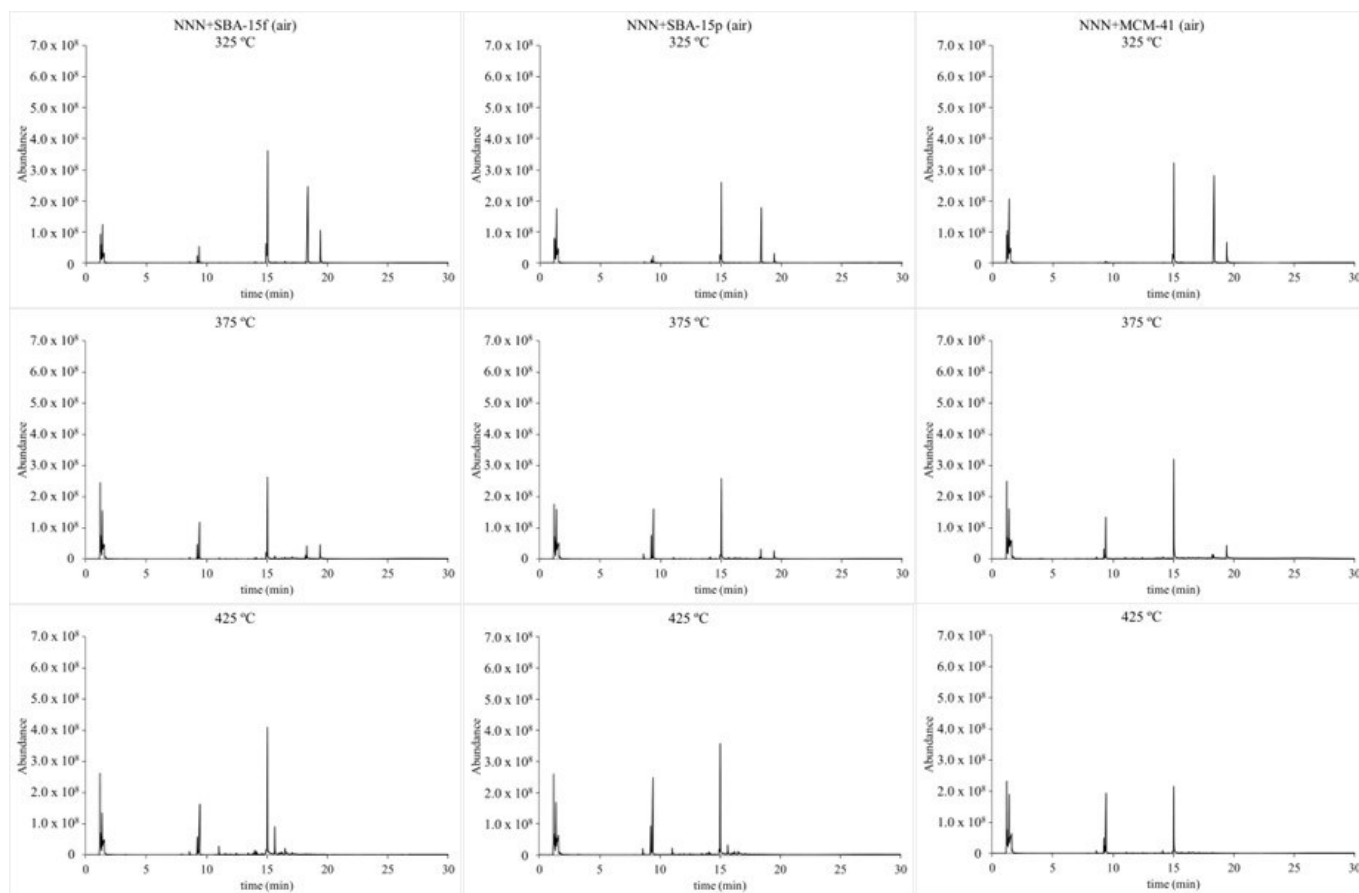


Figure 14. Chromatograms of the pyrolysis of NNN with SBA-15f (left), SBA-15p (center) and MCM-41 (right) at different temperatures, under the air atmosphere.

Appendix Table A3 shows the % area of the different peaks obtained at the three selected temperatures for the three catalysts under the air atmosphere.

Figure 15 shows the evolution of NNN with temperature for the pyrolysis of sole-NNN, as well as with three catalysts, under the air atmosphere.

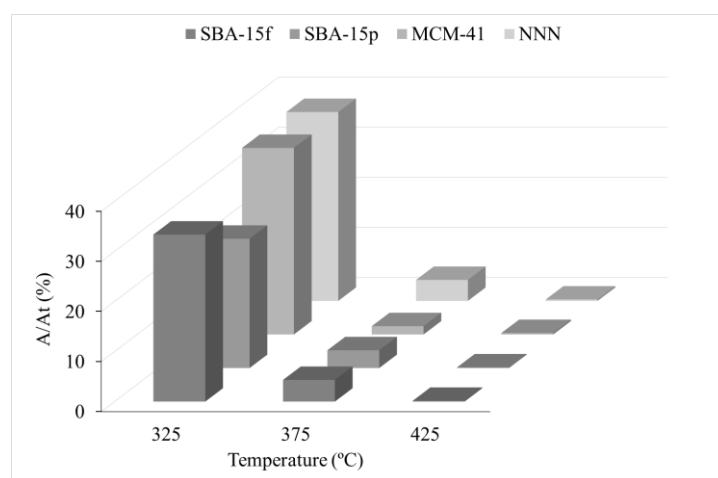


Figure 15. Evolution of NNN for sole NNN and NNN with the three catalysts under air atmosphere.

SBA-15p is the catalysts that produces the largest reduction in NNN at 300 °C, where some reduction is observed for the other two catalysts. Nevertheless, this reduction in the NNN decomposition is less significant than under the inert conditions.

Figure 16 shows the evolution of the main compounds detected with temperature for the three catalysts under air atmosphere.

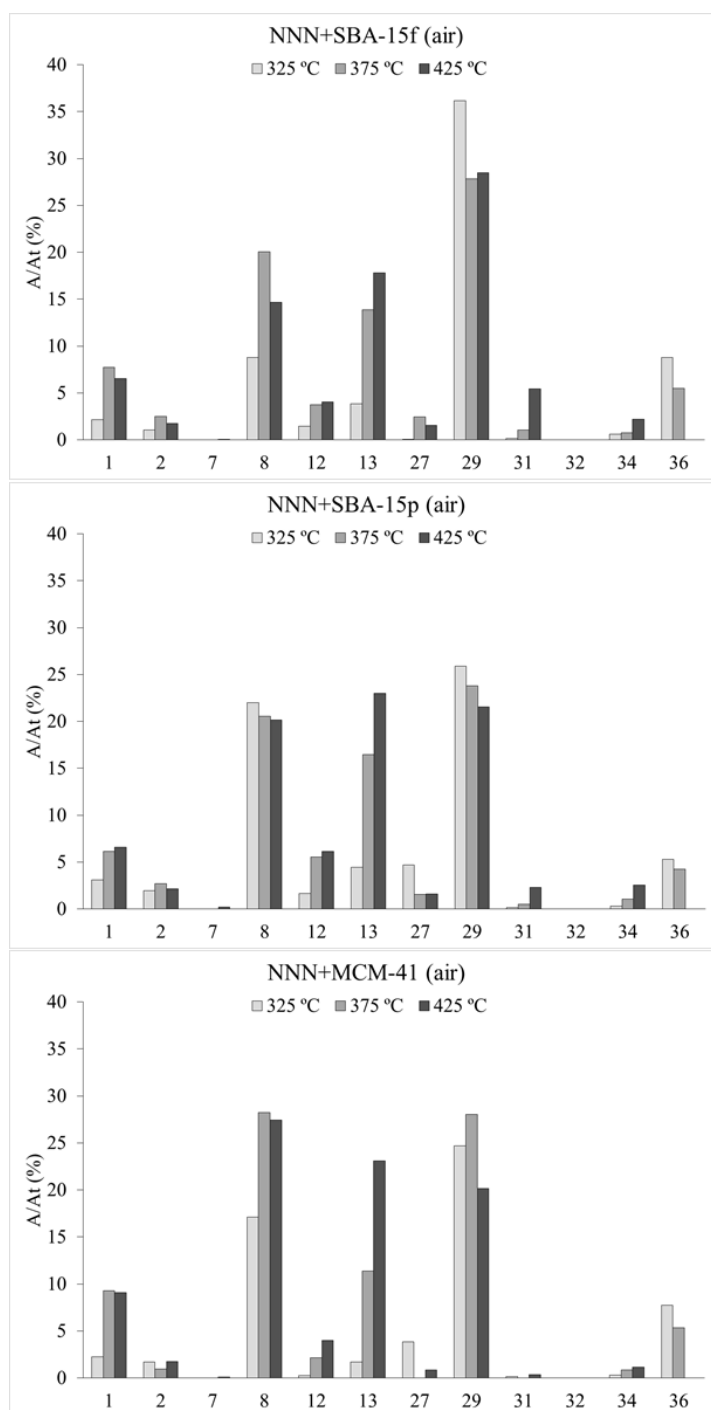


Figure 16. % area vs temperature of the majority compounds detected in the pyrolysis of NNN with three catalysts under air atmosphere. Carbon dioxide (1), nitric oxide (2), formaldehyde (7), water (8), 3-pyridinecarboxaldehyde (12), 3-pyridinecarbonitrile (13), 1H-pyrrolo [2,3-b] pyridine (27), myosmine (29), nicotirryne (31), 4-pyridinecarboxamide (32), nornicotirryne (34) y 5,6-dimethyl-3H-pyrrolo [2,3-b] pyridine (36).

The main effect observed is the large increase in water (compound 8) at all temperatures, going from 6% at 425 °C for NNN to up to 27.4% when using MCM-41. Almost no water was detected in the experiments under the inert atmosphere. Carbon dioxide

(compound 1) is also favored in the presence of the catalysts, showing that the catalysts promote the total oxidation of the NNN and its products of decomposition. Another important effect produced by the presence of catalysts is the decrease of myosmine (compound 29) and 3-pyridinecarbonitrile (compound 13) at high temperatures.

Table 2 shows, in a qualitative manner, the effect of the three catalysts used on the potential toxicity of the products generated in tobacco smoke. This table refers to some selected compounds collected in the Appendix A. The products have been selected according to their potential hazards that lead to their inclusion in different lists in the literature [1], and are present in tobacco smoke. The arrows indicate the sign of the modification produced by the catalysts.

Table 2. Toxic compounds present in the gas generated in the pyrolysis of NNN under both atmospheres.

		SBA-15f		SBA-15p		MCM-41	
		He	air	He	air	He	air
5	<i>Hydrogen cyanide</i>	-	↑	-	↑	-	↑
6	<i>Acetaldehyde</i>	-	↓	-	↑	-	↑
7	<i>Formaldehyde</i>	-	↓	-	↓	-	↓
9	<i>Propanenitrile</i>	↓	-	↓	-	↓	-
10	<i>Pyridine</i>	↓	-	↑	-	↑	-
11	<i>3-ethenyl-pyridine</i>	↓	↓	↑	↑	↑	↓
24	<i>Nicotine</i>	↑	-	↑	-	↑	-
35	<i>NNN</i>	↓	↓	↓	↓	↓	↓

Despite the effects commented on for the different products, this table shows that the more effective catalyst for reducing the presence of toxic compounds is SBA-15f, that reduces all compounds except for hydrogen cyanide (under the air atmosphere) and nicotine (under the inert atmosphere). Nevertheless, the reduction in NNN is much greater for the other two catalysts, and the overall reduction in toxicity may be similar for the three catalysts.

4. Conclusions

This study, developed in the absence and presence of three catalysts, has made it possible to highlighting a series of conclusions that are shown below:

- According to the TG-FTIR analysis of NNN, two main processes of weight loss can be observed. The peaks appears 10 °C before when running the analysis under oxidizing atmosphere, where the main gases analyzed by FTIR show the characteristic band of C=C and the presence of CO₂.
- The presence of the three catalysts has produced modifications in the temperature and intensity of the observed processes, mainly under oxidizing conditions, where the three materials present a third process of weight loss due to the oxidation of the residue. The three materials, mainly MCM-41, show increased IR signals corresponding to CO and CO₂ at temperatures in the range of the third process.
- NNN decomposes at lower temperatures under an oxidizing atmosphere than under an inert atmosphere in the EGA equipment. During the NNN pyrolysis under the inert atmosphere, the main compounds obtained were 3-pyridinecarbonitrile, myosmine and nornicotine. Meanwhile, under the oxidizing atmosphere, the main compounds obtained are 3-pyridinecarbonitrile, myosmine and 5,6-dimethyl-3H-pyrrolo [2,3-b] pyridine, along with CO₂ and water as products of the oxidative degradation of different organic molecules.
- The three catalysts reduce the contribution of the NNN to the total area for both atmospheres in the flash pyrolysis of NNN, especially under inert atmosphere. SBA-15p and SBA-15f highly reduce the contribution of NNN to the total area, especially under the inert atmosphere. However, MCM-41 shows a smaller total area than both SBA-15,

as well as a lower presence of decomposition products and NNN in the chromatograms, in good agreement with the higher residue observed in the TGA experiments.

- The three materials studied strongly modify the product distribution of the gases generated during the pyrolysis of NNN, especially under the oxidizing atmosphere, with 3-pyridinecarbonitrile and myosmine being the two major compounds. For example, myosmine contribution is reduced in the air atmosphere when using SBA-15p and MCM-41. This type of behavior must be due to the higher external specific surface area, pore size and pore volume, resulting in a greater accessibility of the NNN molecule to the porosity of this material. Although the pore size of MCM-41 is significantly smaller, as well as the external area, its highest total area and, mainly, its acidity, may justify its good behavior, better than that of the SBA-15f.
- Nevertheless, SBA-15f is the catalysts yielding the largest reduction in toxic compounds highlighted from the Hoffman list and generated in the pyrolysis of NNN.

Author Contributions: Conceptualization, A.M., M.I.B. and J.A.; Methodology, A.M., M.I.B. and J.A.; Validation, A.M., M.I.B. and J.A.; Investigation, J.A.; Resources, A.M.; Data Curation, A.M., M.I.B., D.B. and J.A.; Writing—Original Draft Preparation, J.A., A.M. and N.J.-S.; Writing—Review and Editing, N.J.-S. and A.M.; Visualization, A.M., M.I.B. and J.A.; Supervision, A.M. and M.I.B.; Project Administration, A.M.; Funding Acquisition, A.M. All authors have read and agreed to the published version of the manuscript.

Funding: Financial support for this investigation has been provided by the “Conselleria d’Educació, Investigació, Cultura i Esport” (grant numbers IDIFEDER 2018/009 and PROMETEO2020/093).

Institutional Review Board Statement: Not applicable.

Informed Consent Statement: Not applicable.

Acknowledgments: The authors wish to thank the “Conselleria d’Educació, Investigació, Cultura i Esport” (grant numbers IDIFEDER 2018/009 and PROMETEO2020/093) for their financial support.

Conflicts of Interest: The authors declare no conflict of interest.

Appendix A

Table A1. Contribution of total area (%) of assigned compounds in the pyrolysis of NNN under inert and oxidizing atmospheres at different temperatures (°C).

#	Assignment #####	Inert Atmosphere			Oxidizing Atmosphere					
		300	400	500	300	325	350	375	400	425
1	Carbon dioxide	-	-	-	0.6	0.9	1.7	3.4	4.4	5.2
2	Nitric oxide	0.4	1.9	6.6	0.6	0.6	1.1	1.2	2	1.5
3	1-propene	-	0.3	0.9	-	-	-	-	-	-
4	Methyl nitrite	-	-	-	0.1	-	0.1	0.1	-	0.2
5	Hydrogen cyanide	-	-	-	-	0.1	0.3	0.4	0.6	0.6
6	Acetaldehyde	-	-	-	-	-	0.1	0.1	0.2	0.3
7	Formaldehyde	-	-	-	0.1	0.3	0.5	1.5	1.4	1.7
8	Water	-	-	-	1.5	2.2	4.2	5.8	6.2	6.6
9	Propanenitrile	-	0.4	0.7	-	-	-	-	-	-
10	Pyridine	-	-	0.1	-	-	-	-	-	-
11	3-ethenyl-pyridine	0.2	0.4	0.9	0.1	0.2	0.4	0.8	1.2	1.3
12	3-pyridinecarboxaldehyde	-	-	-	0.3	0.5	2.1	3.6	5.7	5.8
13	3-pyridinecarbonitrile	0.3	7.1	23	1.1	2.1	8.3	14.4	22.8	28.2
14	1-(3-pyridinyl)-ethanone	-	-	-	-	-	0.1	0.2	0.3	0.3
15	3-pyrindol	-	-	-	-	-	0.3	0.9	1.2	1.4
16	1-(3-pyridinyl)-1-propanone	-	-	-	-	0.1	0.2	0.6	0.7	0.6
17	Niacin	-	-	-	-	0.1	-	0.3	0.3	0.6
18	4-ethenyl-pyridine	0.1	0.3	0.4	-	-	-	-	-	-

Table A1. Cont.

#	Assignment #####	Inert Atmosphere			Oxidizing Atmosphere					
		300	400	500	300	325	350	375	400	425
19	3-methyl-1H-indole	-	-	-	-	-	-	-	-	-
20	4-methyl-1H-indole	-	-	-	-	-	-	-	-	-
21	Isoquinoline	-	-	-	-	-	-	-	-	-
22	3-(4-pyridyl)acrylaldehyde	-	-	-	0.2	0.2	0.3	0.5	0.7	0.6
23	4-methyl-1,5-Naphthyridine	-	-	-	-	-	0.2	0.5	0.5	0.5
24	Nicotine	-	0.1	0.2	-	-	-	-	-	-
25	N-(2-pyridinylmethylene)-1-butanamine	-	0.3	1.7	-	-	-	-	-	-
26	Niacinamide	-	-	-	-	-	0.2	0.7	1.4	1.9
27	1H-pyrrolo [2,3-b]pyridine	3.2	12.7	12.6	10	9.2	8.2	3.6	1.2	0.6
28	Nornicotine	5.9	16.8	12.1	-	-	-	-	-	-
29	Myosmine	10.3	26.5	27.1	25.8	30.1	30.4	36.2	36.9	28.8
30	3,4-dimethyl-pyrrolo(1,2-a)pyrazine	0.1	1.5	3.4	-	-	-	-	-	-
31	Nicotiryn	-	-	-	-	-	-	0.1	0.1	0.1
32	4-pyridinecarboxamide	-	-	-	-	0.2	0.7	2.3	2.1	1.8
33	N-propylnornicotine	-	0.1	0.6	-	-	-	-	-	-
34	Nornicotiryn	-	1.8	0.5	0.5	0.6	0.8	1.5	1.4	1
35	NNN	79.5	27.5	-	47.2	37.7	21.8	4.2	0.4	0.3
36	5,6-dimethyl-3H-pyrrolo [2,3-b]pyridine	-	-	-	10.2	12.3	13.9	6.5	0.2	0.2

Table A2. Contribution of total area (%) of assigned compounds in the catalytic pyrolysis of NNN with three catalyst under the inert atmosphere at different temperatures (°C).

#	Assignment #####	NNN+SBA-15f			NNN+SBA-15p			NNN+MCM-41		
		300	400	500	300	400	500	300	400	500
1	Carbon dioxide	-	-	-	-	-	-	-	-	-
2	Nitric oxide	2.6	2.3	4.1	4.6	3.7	4.2	1.7	6.2	6.9
3	1-propene	0.4	0.1	0.3	0.3	0.3	0.4	0.2	0.6	0.8
4	Methyl nitrite	-	-	-	-	-	-	-	-	-
5	Hydrogen cyanide	-	-	-	-	-	-	-	-	-
6	Acetaldehyde	-	-	-	-	-	-	-	-	-
7	Formaldehyde	-	-	-	-	-	-	-	-	-
8	Water	-	-	-	-	-	-	-	-	-
9	Propanenitrile	-	0.1	0.3	-	0.1	0.1	-	0.2	0.3
10	Pyridine	-	-	0.1	-	-	0.2	-	-	0.7
11	3-ethenyl-pyridine	0.8	0.8	0.4	2.4	1.2	1.8	1.1	3.3	3.9
12	3-pyridinecarboxaldehyde	-	-	-	-	-	-	-	-	-
13	3-pyridinecarbonitrile	0.2	3.9	4.5	0.1	2.2	5.7	-	4.6	10.7
14	1-(3-pyridinyl)-ethanone	-	-	-	-	-	-	-	-	-
15	3-pyrindol	-	-	-	-	-	-	-	-	-
16	1-(3-pyridinyl)-1-propanone	-	-	-	-	-	-	-	-	-
17	Niacin	-	-	-	-	-	-	-	-	-
18	4-ethenyl-pyridine	0.8	0.6	0.7	0.2	0.3	0.4	0.1	0.4	0.4
19	3-methyl-1H-indole	-	0.1	0.2	-	0.1	0.4	-	0.2	0.9
20	4-methyl-1H-indole	-	0.1	0.2	-	-	0.5	-	0.4	0.8
21	Isoquinoline	-	-	0.1	-	-	0.2	-	0.2	1.2
22	3-(4-pyridyl)acrylaldehyde	-	-	-	-	-	-	-	-	-
23	4-methyl-1,5-Naphthyridine	-	-	-	-	-	-	-	-	-
24	Nicotine	1.1	0.2	0.4	0.1	0.4	0.9	0.1	0.5	1.3
25	N-(2-pyridinylmethylene)-1-butanamine	-	0.2	0.9	-	0.1	0.2	-	0.1	0.6
26	Niacinamide	-	-	-	-	-	-	-	-	-
27	1H-pyrrolo [2,3-b]pyridine	10.7	15.6	15.7	9.1	13.3	13.9	2.7	8.3	8.6
28	Nornicotine	12.5	17.6	16.4	17.7	22.6	17.0	4.4	10.6	6.7
29	Myosmine	26.2	34.1	43.0	26.0	39.1	42.6	14.3	34.1	40.7
30	3,4-dimethyl-pyrrolo(1,2-a)pyrazine	-	0.5	1.0	-	-	0.3	-	-	0.6

Table A2. Cont.

#	Assignment #####	NNN+SBA-15f			NNN+SBA-15p			NNN+MCM-41		
		300	400	500	300	400	500	300	400	500
31	Nicotirylene	0.3	0.2	0.6	-	0.6	0.5	-	0.8	1.2
32	4-pyridinecarboxamide	-	-	-	-	-	-	-	-	-
33	N-propylornicotine	-	0.1	0.2	-	0.1	0.1	-	-	0.1
34	Normicotirylene	0.5	1.9	3.3	1.1	3.9	5.2	-	2.4	5.6
35	NNN	43.2	19.4	-	37.9	10.7	-	75.3	25.7	-
36	5,6-dimethyl-3H-pyrrolo [2,3-b]pyridine	-	-	-	-	-	-	-	-	-

Table A3. Contribution of total area (%) of assigned compounds in the catalyst pyrolysis of NNN with three catalyst under the air atmosphere at different temperatures (°C).

#	Assignment #####	NNN+SBA-15f			NNN+SBA-15p			NNN+MCM-41		
		325	375	425	325	375	425	325	375	425
1	Carbon dioxide	2.2	7.7	6.5	3.1	6.1	6.6	2.3	9.3	9.1
2	Nitric oxide	1.1	2.5	1.8	2	2.7	2.2	1.7	1	1.8
3	1-propene	-	-	-	-	-	-	-	-	-
4	Methyl nitrite	-	-	0.9	-	1.4	0.4	-	0.2	0.6
5	Hydrogen cyanide	0.4	0.8	0.5	0.5	0.5	1.1	0.8	0.6	0.4
6	Acetaldehyde	0.2	0.1	0.2	0.1	0.4	0.2	0.2	0.8	0.5
7	Formaldehyde	-	-	-	-	-	0.2	-	-	0.1
8	Water	8.8	20.1	14.7	22	20.6	20.2	17.1	28.2	27.4
9	Propanenitrile	-	-	-	-	-	-	-	-	-
10	Pyridine	-	-	-	-	-	-	-	-	-
11	3-ethenyl-pyridine	0.3	0.6	0.7	0.8	1.5	1.5	-	0.9	1
12	3-pyridinecarboxaldehyde	1.4	3.8	4	1.7	5.6	6.2	0.3	2.1	4
13	3-pyridinecarbonitrile	3.8	13.9	17.8	4.4	16.5	23	1.7	11.4	23.1
14	1-(3-pyridinyl)-ethanone	0.1	0.6	1.7	0.2	0.9	1.6	-	0.4	0.6
15	3-pyrindol	-	-	-	-	-	-	-	-	-
16	1-(3-pyridinyl)-1-propanone	0.1	0.2	0.3	-	0.2	0.3	-	0.3	0.3
17	Niacin	-	-	-	-	-	-	-	-	-
18	4-ethenyl-pyridine	-	-	-	-	-	-	-	-	-
19	3-methyl-1H-ndole	-	-	-	-	-	-	-	-	-
20	4-methyl-1H-indole	-	-	-	-	-	-	-	-	-
21	Isoquinoline	-	-	-	-	-	-	-	-	-
22	3-(4-pyridyl)acrylaldehyde	0.4	0.4	0.8	-	0.3	0.4	-	0.2	0.4
23	4-methyl-1,5-Naphthyridine	0.1	0.5	0.5	0.1	0.6	0.5	-	0.3	0.8
24	Nicotine	-	-	-	-	-	-	-	-	-
25	N-(2-pyridinylmethylene)-1-butanamine	-	-	-	-	-	-	-	-	-
26	Niacinamide	-	0.2	0.7	-	-	-	-	-	-
27	1H-pyrrolo [2,3-b]pyridine	-	2.5	1.5	4.7	1.6	1.6	3.9	-	0.9
28	Normicotine	-	-	-	-	-	-	-	-	-
29	Myosmine	36.2	27.9	28.5	25.9	23.8	21.6	24.7	28	20.1
30	3,4-dimethyl-pyrrolo(1,2-a)pyrazine	-	-	-	-	-	-	-	-	-
31	Nicotirylene	0.2	1.1	5.4	0.2	0.5	2.3	0.2	-	0.4
32	4-pyridinecarboxamide	-	-	-	-	-	-	-	-	-
33	N-propylornicotine	-	-	-	-	-	-	-	-	-
34	Normicotirylene	0.6	0.8	2.2	0.3	1.1	2.6	0.3	0.9	1.2
35	NNN	33.4	4.3	0.2	25.8	3.6	0.1	37.3	1.7	0.3
36	5,6-dimethyl-3H-pyrrolo [2,3-b]pyridine	8.8	5.5	-	5.3	4.2	-	7.7	5.3	-

References

- Hoffmann, D.; Hoffmann, I. Tobacco smoke components. *Beitr. Tab. Int.* **1998**, *18*, 49–52.
- Thielen, A.; Klus, H.; Müller, L. Tobacco smoke: Unraveling a controversial subject. *Exp. Toxicol. Pathol.* **2008**, *60*, 141–156. [[CrossRef](#)]

3. Borgerding, M.; Klus, H. Analysis of complex mixtures—cigarette smoke. *Exp. Toxicol. Pathol. Off. J. Ges. Toxikol. Pathol.* **2005**, *57* (Suppl. S1), 43–73. [[CrossRef](#)] [[PubMed](#)]
4. Hecht, S.S.; Szabo, E. Fifty years of tobacco carcinogenesis research: From mechanisms to early detection and prevention of lung cancer. *Cancer Prev. Res.* **2014**, *7*, 1–8. [[CrossRef](#)] [[PubMed](#)]
5. U.S. Department of Health and Human Services. *The Health Consequences of Smoking—50 Years of Progress: A Report of the Surgeon General*; Centers for Disease Control and Prevention (US): Atlanta, GA, USA, 2014.
6. National Toxicology Program (NTP). *Report on Carcinogens*, 14th ed.; U.S. Department of Health and Human Services, Public Health Service: Research Triangle Park, NC, USA, 2016.
7. Reynolds, B.; McGarvey, B.; Todd, J. Agronomics of high density tobacco (*Nicotiana tabacum*) production for protein and chemicals in Canada. *Biocatal. Agric. Biotechnol.* **2022**, *42*, 102357. [[CrossRef](#)]
8. Zou, X.; Amrit, B.K.; Abu-Izneid, T.; Aziz, A.; Devnath, P.; Rauf, A.; Mitra, S.; Bin Emran, T.; Mujawah, A.A.H.; Lorenzo, J.M.; et al. Current advances of functional phytochemicals in *Nicotiana* plant and related potential value of tobacco processing waste: A review. *Biomed. Pharmacother.* **2021**, *143*, 112191. [[CrossRef](#)] [[PubMed](#)]
9. Bareschino, P.; Marrasso, E.; Roselli, C. Tobacco stalks as a sustainable energy source in civil sector: Assessment of techno-economic and environmental potential. *Renew. Energy.* **2021**, *175*, 373–390. [[CrossRef](#)]
10. Hoffmann, D.; Hecht, S.S. Advances in Tobacco Carcinogenesis. In *Chemical Carcinogenesis and Mutagenesis I*; Cooper, C.S., Grover, P.L., Eds.; Springer: Berlin/Heidelberg, Germany, 1990; pp. 63–102. [[CrossRef](#)]
11. Hecht, S. *Metabolism of Carcinogenic Tobacco-Specific Nitrosamines*; University of Minnesota Twin Cities: Minneapolis, MN, USA, 2012; pp. 2–3.
12. Hecht, S.S. Tobacco carcinogens, their biomarkers and tobacco-induced cancer. *Nat. Rev. Cancer* **2003**, *3*, 733–744. [[CrossRef](#)]
13. Takahashi, H.; Ogata, H.; Nishigaki, R.; Broide, D.H.; Karin, M. Tobacco Smoke Promotes Lung Tumorigenesis by Triggering IKK β - and JNK1-Dependent Inflammation. *Cancer Cell* **2010**, *17*, 89–97. [[CrossRef](#)]
14. Fischer, S.; Spiegelhalder, B.; Eisenbarth, J.; Preussmann, R. Investigations on the origin of tobacco-specific nitrosamines n mainstream smoke of cigarettes. *Carcinogenesis* **1990**, *11*, 723–730. [[CrossRef](#)] [[PubMed](#)]
15. Hu, Z.; Liao, Z.; Deng, Q.; Huang, Y.; Xie, W.; Lin, Y.; Huang, H.; Ma, P.; Li, Y.; Li, Q.; et al. Analysis the formation of 4-(methylnitrosamino)-1-(3-pyridyl)-1-butanone in tobacco smoke generated from pyrolysis under inert and oxidative conditions respectively. *J. Anal. Appl. Pyrolysis* **2017**, *127*, 75–81. [[CrossRef](#)]
16. Sophia, F.; Spiegelhalder, B.; Preussmann, R. Preformed tobacco-specific nitrosamines in tobacco—Role of nitrate and influence of tobacco type. *Carcinogenesis* **1989**, *10*, 1511–1517. [[CrossRef](#)] [[PubMed](#)]
17. Hecht, S.S.; Chen, C.-H.B.; Ornaf, R.M.; Jacobs, E.; Adams, J.D.; Hoffmann, D. Reaction of Nicotine and Sodium Nitrite: Formation of Nitrosamines and Fragmentation of the Pyrrolidine Ring. *J. Org. Chem.* **1978**, *43*, 72–76. [[CrossRef](#)] [[PubMed](#)]
18. Adams, J.D.; Lee, S.J.; Vinchkoski, N.; Castonguay, A.; Hoffmann, D. On the formation of the tobacco-specific carcinogen 4-(methylnitrosamino)-1-(3-pyridyl)-1-butanone during smoking. *Cancer Lett.* **1983**, *17*, 339–346. [[CrossRef](#)]
19. Brunnemann, K.D.; Hoffmann, D. Analytical Studies on Tobacco-Specific N-Nitrosamines in Tobacco and Tobacco Smoke. *Crit. Rev. Toxicol.* **1991**, *21*, 235–240. [[CrossRef](#)] [[PubMed](#)]
20. Yun, Z.Y.; Xu, Y.; Xu, J.H.; Wu, Z.Y.; Wei, Y.L.; Zhou, Z.P.; Zhu, J.H. In situ FTIR investigation on the adsorption of nitrosamines in zeolites. *Microporous Mesoporous Mater.* **2004**, *72*, 127–135. [[CrossRef](#)]
21. Zhou, C.F.; Cao, Y.; Zhuang, T.T.; Huang, W.; Zhu, J.H. Capturing Volatile Nitrosamines in Gas Stream by Zeolites: Why and How. *J. Phys. Chem. C.* **2007**, *111*, 4347–4357. [[CrossRef](#)]
22. Zhou, C.F.; Yun, Z.Y.; Xu, Y.; Wang, Y.M.; Chen, J.; Zhu, J.H. Adsorption and room temperature degradation of N-nitrosodiphenylamine on zeolites. *New J. Chem.* **2004**, *28*, 807. [[CrossRef](#)]
23. Zhu, J.H.; Yan, D.; Rong Xai, J.; Ma, L.L.; Shen, B. Attempt to adsorb N-nitrosamines in solution by use of zeolites. *Chemosphere* **2001**, *44*, 949–956. [[CrossRef](#)]
24. Zhou, C.F.; Zhu, J.H. Adsorption of nitrosamines in acidic solution by zeolites. *Chemosphere* **2005**, *58*, 109–114. [[CrossRef](#)] [[PubMed](#)]
25. Gao, L.; Cao, Y.; Zhou, S.L.; Zhuang, T.T.; Wang, Y.; Zhu, J.H. Eliminating carcinogenic pollutants in environment: Reducing the tobacco specific nitrosamines level of smoke by zeolite-like calcosilicate. *J. Hazard. Mater.* **2009**, *169*, 1034–1039. [[CrossRef](#)]
26. Lin, W.G.; Zhou, Y.; Cao, Y.; Zhou, S.L.; Wan, M.M.; Wang, Y.; Zhu, J.H. Applying heterogeneous catalysis to health care: In situ elimination of tobacco-specific nitrosamines (TSNAs) in smoke by molecular sieves. *Catal. Today* **2013**, *212*, 52–61. [[CrossRef](#)]
27. Cao, Y.; Yun, Z.Y.; Yang, J.; Dong, X.; Zhou, C.F.; Zhuang, T.T.; Yu, Q.; Liu, H.D.; Zhu, J.H. Removal of carcinogens in environment: Adsorption and degradation of N'-nitrosornicotine (NNN) in zeolites. *Microporous Mesoporous Mater.* **2007**, *103*, 352–362. [[CrossRef](#)]
28. Cheng, J.-P.; Xian, M.; Wang, K.; Zhu, X.; Yin, Z.; Wang, P.G. Heterolytic and Homolytic Y–NO Bond Energy Scales of Nitroso-Containing Compounds: Chemical Origin of NO Release and NO Capture. *J. Am. Chem. Soc.* **1998**, *120*, 10266–10267. [[CrossRef](#)]
29. Tanno, M.; Sueyoshi, S.; Miyata, N.; Nakagawa, S. Nitric Oxide Generation from Aromatic N-Nitrosoureas at Ambient Temperature. *Chem. Pharm. Bull.* **1996**, *44*, 1849–1852. [[CrossRef](#)]
30. Gómez-Siurana, A.; Marcilla, A.; Beltrán, M.; Berenguer, D.; Martínez-Castellanos, I.; Menargues, S. TGA/FTIR study of tobacco and glycerol–tobacco mixtures. *Thermochim. Acta* **2013**, *573*, 146–157. [[CrossRef](#)]

31. Marcilla, A.; Gomez Siurana, A.; Beltran Rico, M.I.; Martinez Castellanos, I.; Berenguer Muñoz, D. Aluminosilicato SAB-15 Como Aditivo para la Reducción de los Compuestos Tóxicos y Cancerígenos Presentes en el Humo del Tabaco. WIPO Patent WO2014096486A1, 26 June 2014.
32. Marcilla, A.; Beltran, M.I.; Gómez-Siurana, A.; Martínez-Castellanos, I.; Berenguer, D.; Pastor, V.; García, A.N. TGA/FTIR study of the pyrolysis of diammonium hydrogen phosphate–tobacco mixtures. *J. Anal. Appl. Pyrolysis* **2015**, *112*, 48–55. [[CrossRef](#)]
33. Marcilla, A.; Beltran, M.; Gómez-Siurana, A.; Berenguer, D.; Martínez-Castellanos, I. Nicotine/mesoporous solids interactions at increasing temperatures under inert and air environments. *J. Anal. Appl. Pyrolysis* **2016**, *119*, 162–172. [[CrossRef](#)]
34. Marcilla, A.; Beltran, M.; Gómez-Siurana, A.; Martínez, I.; Berenguer, D.; Gomis, A.; Beltrán, M.; Siurana, A.; Martínez, I.; Berenguer, D. Catalytic effect of MCM-41 on the pyrolysis and combustion processes of tobacco. *Eff. Alum. Content. Thermochim. Acta* **2011**, *518*, 47–52. [[CrossRef](#)]
35. Asensio, J.; Beltrán, M.I.; Marcilla, A. Nicotine Fast Pyrolysis Under Inert and Air Environments. Effect of Catalysts. *J. Anal. Appl. Pyrolysis*, 2022; *submitted*. [[CrossRef](#)]
36. Zhao, D.; Zhang, F.; Tu, B.; Yang, H.; Yu, C.; Yan, Y.; Meng, Y. Understanding Effect of Wall Structure on the Hydrothermal Stability of Mesoporous Silica SBA-15. *J. Phys. Chem. B* **2005**, *109*, 8723–8732. [[CrossRef](#)]
37. Yeh, Y.Q.; Lin, H.P.; Tang, C.Y.; Mou, C.Y. Mesoporous silica SBA-15 sheet with perpendicular nanochannels. *J. Colloid Interface Sci.* **2011**, *362*, 354–366. [[CrossRef](#)]
38. Gaydhankar, T.R.; Samuel, V.; Jha, R.K.; Kumar, R.; Joshi, P.N. Room temperature synthesis of Si-MCM-41 using polymeric version of ethyl silicate as a source of silica. *Mater. Res. Bull.* **2007**, *42*, 1473–1484. [[CrossRef](#)]
39. Asensio, J. Pirólisis Térmica y Catalítica de la Nicotina y NNK y NNN, dos Nitrosaminas Específicas del Tabaco. Ph.D. Defended Thesis, Universidad de Alicante, Alicante, Spain, 2020.
40. Wei, F.; Gu, F.N.; Zhou, Y.; Gao, L.; Yang, J.; Zhu, J.H. Modifying MCM-41 as an efficient nitrosamine trap in aqueous solution. *Solid State Sci.* **2009**, *11*, 402–410. [[CrossRef](#)]
41. Zhu, J.H.; Zhou, S.L.; Xu, Y.; Cao, Y.; Wei, Y.-L. Ordered Mesoporous Materials. Novel Catalyst for Degradation of N'-Nitrosornicotine. *Chem. Lett.* **2003**, *32*, 338–339. [[CrossRef](#)]
42. Li, Y.Y.; Wan, M.M.; Zhu, J.H. Cleaning carcinogenic nitrosamines with zeolites. *Environ. Chem. Lett.* **2014**, *12*, 139–152. [[CrossRef](#)]